CsTl: A New Example of Tetragonally Compressed Tl_6^{6-} Octahedra. Electronic Effects and Packing Requirements in the Diverse Structures of ATl (A = Li, Na, K, Cs)

Zhen-Chao Dong and John D. Corbett*

Ames Laboratory—DOE[1] and Department of Chemistry, Iowa State University, Ames, Iowa 50011

Received September 29, 1995[⊗]

The cesium-richest phase in the Cs−Tl system, CsTl, can be isolated as a pure crystalline phase through slow cooling of cesium-richer compositions in Ta followed by vacuum sublimation of the excess Cs at ∼100 °C. The compound melts incongruently in the neighborhood of 150 °C. The structure was established by single crystal X-ray diffraction at room temperature (orthorhombic *Fddd*, $Z = 48$, $a = 32.140(3)$ Å, $b = 15.136(1)$ Å, and $c = 9.2400(7)$ Å. The isolated Tl_6^{6-} ions in the structure, tetragonally compressed octahedra, exhibit D_2 symmetry with ≤0.063(4) Å differences in edge lengths from D_{4h}. Extended Hückel calculations confirm the classical nature of the distortion in lowering the cluster electron count and charge. The diamagnetic CsTl differs from KTl, which contains more distorted Tl_6^{6-} ions (C_{2h}), in a doubled *a* axis and an additional interpenetrating cluster anion sublattice. The smaller distortion of the clusters in CsTl originates with the lower field of the same number of cation neighbors in a more symmetric arrangement. The structural trend from LiTl (CsCl type) through the classic NaTl (stuffed diamond) to the related KTl and CsTl with compressed octahedra (and the absence of any such Rb phase) relates to the efficient packing of A^+ and $(Tl^-)_n$ over a widely varying range of A^+ sizes, with only Na^+ fitting well within a $^3_\infty(Tl^-)$ lattice. Similarly 4-bonded thallium in KTl and CsTl with somewhat shorter Tl−Tl distances is a necessary alternative when the infinite lattice cannot tolerate larger cations.

Introduction

Thallium has proven to be extremely prolific in the number of cluster anions that it forms, and cation size factors are crucial in delineating what clusters and compositions are found in many alkali-metal−thallium compounds. A single cation type in the binary systems yields only three kinds of isolated thallium clusters, Tl_4^{8-} only in Na_2Tl,[2] Tl_6^{6-} in orthorhombic KTl,[3] and the present CsTl and Tl_{11}^{7-} in A_8Tl_{11} (A = K, Rb, Cs)[4,5] and $A_{15}Tl_{27}$ (A = Rb, Cs).[6] On the other hand, mixed cations provide more flexibility for the efficient packing of cations and polyanions coupled with electronic requirements for what are usually closed-shell anions. Five more discrete thallium clusters have been so discovered just in systems in which Na is mixed with K, Rb, or Cs: Tl_3^{7-}, Tl_5^{7-},[7,8] Tl_9^{9-},[8] $Tl_{12}Na^{13-}$,[9] Tl_{13}^{10-} and Tl_{13}^{11-}.[10] Further size and electronic tuning among cluster anions can also be accomplished through the inclusion of an appropriate heterometal, either substitutionally or interstitially.[7,11,12] Close sheaths of cations about cluster faces, edges, and vertices throughout these give space-filling structures and appear to be critical in stabilizing what are probably relatively soft polyanions.

Following the characterization of compressed ($\sim D_{2h}$) Tl_6^{6-} units in KTl,[3] regular (O_h) and more reduced Tl_6^{8-} units have been discovered in $Na_{14}K_6Tl_{18}M$ (M = Mg, Zn−Hg) in conjunction with M-centered icosahedra.[12] The only other example of a "naked" and fairly regular octahedron is Ga_6 recently found in Ba_5Ga_6[13] (which is actually the hydride, $Ba_5Ga_6H_2$[14,15]). In contrast, exo-bonded or ligated octahedral clusters are typical units among the transition-metal and rare-earth-metal cluster halides and chalcogenides,[16,17] as well as for main-group elements, e.g., in $B_6H_6^{2-}$,[18] $C_2B_4H_6$,[19] and $Sn_6(Cr(CO)_5)_6^{2-}$,[20] and also interconnected in the hexaborides of Na, K, Ca, and La[21] as well as in layers of A_2In_3 (A = Rb, Cs).[22]

In this article, we report another 1:1 binary A−Tl phase, CsTl, which contains naked, compressed "octahedral" clusters grossly similar to those in KTl[3] but with distinctly different polyanion packing and higher symmetry that emphasize how much the "solvation" of anions by different cations can influence geometry as well as phase stability. This brings to our attention the range of other 1:1 ATl phases that are known, LiTl in a CsCl-type structure[23] and NaTl as the parent stuffed diamond structure.[24] Efforts will be made to explain the structural differences among

⊗ Abstract published in *Advance ACS Abstracts,* March 1, 1996.
(1) This research was supported by the Office of Basic Energy Sciences, Materials Sciences Division, U.S. Department of Energy. Ames Laboratory is operated for DOE by Iowa State University under Contract No. W-7405-Eng-82.
(2) Hansen, D. A.; Smith, J. F. *Acta Crystallogr.* **1967**, *22*, 836.
(3) Dong, Z.-C.; Corbett, J. D. *J. Am. Chem. Soc.* **1993**, *115*, 11299.
(4) Cordier, G.; Müller, V. *Z. Kristallogr.* **1992**, *198*, 281.
(5) Dong, Z.-C.; Corbett, J. D. *J. Cluster Sci.* **1995**, *6*, 187.
(6) Dong, Z.-C.; Corbett, J. D. *Inorg. Chem.*, in press.
(7) Dong, Z.-C.; Corbett, J. D. Unpublished research.
(8) Dong, Z.-C.; Corbett, J. D. *J. Am. Chem. Soc.* **1994**, *116*, 3429.
(9) Dong, Z.-C.; Corbett, J. D. *Inorg. Chem.* **1995**, *34*, 5709.
(10) Dong, Z.-C.; Corbett, J. D. *J. Am. Chem. Soc.* **1995**, *117*, 6447.
(11) Dong, Z.-C.; Corbett, J. D. *Inorg. Chem.* **1995**, *34*, 5042.
(12) Dong, Z.-C.; Corbett, J. D. *Angew. Chem.*, accepted for publication.
(13) Fornasini, M. L.; Pani, M. *J. Alloys Compd.* **1994**, *205*, 179.
(14) Liu, Q.; Hoffmann, R.; Corbett, J. D. *J. Phys. Chem.* **1994**, *98*, 9360.
(15) Henning, R. W.; Leon-Escamilla, E. A.; Zhao, J.-T.; Corbett, J. D. Unpublished research.
(16) Simon, A. *Angew. Chem., Int. Ed. Engl.* ***1988***, *27*, 160.
(17) Corbett, J. D. In *Modern Perspectives in Inorganic Crystal Chemistry*; Parthé, E., Ed.; NATO ASI Series C; Kluwer Academic Publishers: Dordrecht, The Netherlands, 1992; p 27.
(18) Schaeffer, R.; Johnson, Q.; Smith, G. S. *Inorg. Chem.* **1965**, *4*, 917.
(19) Beaudet, R. A.; Poynter, R. L. *J. Chem. Phys.* **1970**, *53*, 1899.
(20) Schiemenz, B.; Huttner, G. *Angew. Chem., Int. Ed. Engl.* **1993**, *32*, 297.
(21) NaB_6: Hagenmuller, P.; Naslain, R. *C. R. Hebd. Seances Acad. Sci.* **1963**, *257*, 1294. KB_6: Naslain, R.; Etourneau, J. *C. R. Seances Acad. Sci., Ser. C* **1966**, *263*, 484. CaB_6: Blum, P.; Bertaut, F. *Acta Crystallogr.* **1954**, *7*, 81. LaB_6: Korsukova, M. M.; Gurin, V. N.; Lundström, T.; Tergenius, L.-E. *J. Less-Common Met.* **1986**, *117*, 73.
(22) Sevov, S. C.; Corbett, J. D. *Z. Anorg. Allg. Chem.* **1993**, *619*, 128.
(23) Pauly, H.; Weiss, A.; Witte, H. *Z. Metallkunde* **1968**, *59*, 554.
(24) Zintl, E.; Dullenkopf, W. *Z. Phys. Chem.* **1932**, *B16*, 195.

0020-1669/96/1335-2301$12.00/0

Table 1. Selected Data Collection and Refinement Parameters for CsTl

fw	337.28	V, Å^3	4495.0(6)
space group, Z	*Fddd*, 48	D_{calc}, g/cm^3	5.980
lattice params,[a] Å		μ, cm^{-1} (Mo Kα)	527.96
a	32.140(3)	residuals: R; R_w[b]	0.043; 0.047
b	15.136(1)		
c	9.2400(7)		

[a] Guinier data, $\lambda = 1.540\,562$ Å, 22 °C. [b] $R = \sum||F_o| - |F_c||/\sum|F_o|$; $R_w = [\sum w(|F_o| - |F_c|)^2/\sum w(F_o)^2]^{1/2}$; $w = 1/\sigma^2$.

the 1:1 series on the basis of packing and the Zintl concept,[25] specifically the cation solvation and anion bonding. Electrical and magnetic properties and their correlations with structure will also be discussed.

Experimental Section

Syntheses. All the syntheses were carried out by fusion of the constituent elements. The surface of the thallium metal bar (99.998%, Johnson-Matthey) was cleaned with a scalpel before use, while the cesium (99.9%, Johnson-Matthey) was used as received, sealed under Ar. The general reaction techniques in welded Ta tubing have been described previously.[8] Because both reagents and products are very sensitive to air and moisture, all operations were performed in a N_2- or He-filled glovebox with a typical humidity level of less than 0.1 ppm (vol.).

The 1:1 CsTl phase is the cesium-richest phase in the binary Cs−Tl system. The 1981 phase diagram reported by Busmanov and Yatsenko on the basis of thermal analyses[26] indicated only a monotectic point at 355 °C at this composition, although all other binary phases were properly identified but with approximate formulations, i.e., Cs_8Tl_{11}[5] as "Cs_5Tl_7", $Cs_{15}Tl_{27}$[6] as "Cs_4Tl_7", and Cs_4Tl_{13}[7] as "$CsTl_3$". The compounds KTl and CsTl alike are neighbors of the congruently melting, Tl-richer A_8Tl_{11} phases, and we have found no other phases on the Cs-richer side of the 1:1 CsTl composition according to powder patterns of samples in this region. For example, a Cs_2Tl mixture equilibrated at 500 °C in Ta followed by slow cooling over 4 days yielded a mixture of the brittle CsTl phase (as well-formed crystals) covered by soft Cs metal with an overall golden appearance. The color changed to dark grey after excess Cs was removed by the following distillation technique. The reaction mixture was transferred into a dumbbell-shaped Pyrex tube long enough to have one end in ice water and the other inside a furnace at ∼100 °C. This was evacuated and sealed. Complete distillation of the Cs took about 2 days and was monitored visually. The well-shaped dark grey crystals were not destroyed during this process. This procedure appears to be the best way to get a pure CsTl phase. High yields were not achieved for stoichiometric reactions by annealing at, typically, 200 or 250 °C for 30 days, which gave a minor CsTl phase, Cs_8Tl_{11} as the major product, and, of course, Cs. The above heating profiles together with their product distributions suggest that, first, CsTl is incongruently melting and, second, its peritectic point is probably around 150 °C, well below the reported monotectic temperature (355 °C). Reactions targeted on RbTl were also run, but no such compound was observed. Guinier powder patterns from all Rb-richer samples showed Rb_8Tl_{11} as the only detectable compound, making it the alkali-metal-richest phase. (The excess Rb (or Cs) metal was not seen in the above powder patterns, which is usual according to our experiences.) There is a cubic K-richer phase ($a = 22.645(4)$ Å) near K_2Tl in composition that we have not been able to characterize well.[7]

X-ray Powder Diffraction. Sharp X-ray powder patterns for CsTl samples mounted between pieces of cellophane were obtained with the aid of an Enraf-Nonius Guinier camera, Cu Kα radiation ($\lambda = 1.540\,56$ Å), and NBS (NIST) silicon as an internal standard. A least-squares refinement for 69 lines indexed on the basis of the refined structural model gave rise to the lattice constants reported in Table 1. CsTl is a line compound judging from the cell parameters from different compositions, which give the same values with deviations of less than 3σ.

Table 2. Positional Coordinates and Isotropic Thermal Parameters for CsTl

atom	x	y	z	B_{eq}[a] (Å^2)
Tl1	0.32161(5)	0.8784(3)	0.0594(2)	2.56(7)
Tl2	1/8	0.5014(2)	1/8	2.8(1)
Cs1	0.2743(1)	1/8	1/8	3.6(2)
Cs2	0.7844(1)	1/8	1/8	3.4(2)
Cs3	1/8	0.2539(3)	1/8	2.9(2)

[a] $B_{eq} = (8\pi^2/3)\sum_i\sum_j U_{ij} a_i^* a_j^* \vec{a}_i \vec{a}_j$.

Magnetic Susceptibilities. Magnetic susceptibility data were obtained from a 38-mg powdered sample held between two fused silica rods, which were in turn fixed inside silica tubing that was sealed at both ends under He. Measurements were made at a field of 3 T over the range of 6−300 K with the aid of a Quantum Design MPMS SQUID magnetometer. The raw data were corrected for the susceptibilities of the containers and the diamagnetism of the cores[27] as well as for the Larmor precession contribution of the delocalized valence electrons in the cluster orbitals, as before.[8,28]

Structure Determination. Laue and oscillation photographs were used to check the singularity of crystals and to gain information about cell dimensions and symmetry. A crystal of ca. 0.10 × 0.10 × 0.13 mm^3, previously sealed in a thin-wall capillary, was chosen and mounted on a Rigaku AFC6R single crystal diffractometer equipped with graphite-monochromated Mo Kα radiation. Programmed indexing of 25 reflections from a random search over $14 \le 2\theta \le 30°$ yielded an face-centered orthorhombic cell. Two octants of data were collected at room temperature with F-centering conditions imposed and were corrected for Lorentz and polarization effects. (The F-centering absences were confirmed during a previous data set collection without constraints that yielded the same structural model but failed to give a good refinement owing to a poor crystallinity and an insufficient number of observed reflections.) Intensity data show systematic absences consistent with the space group *Fddd*, which was then used in the first trial and proven to be correct by the subsequent successful refinement. The structure was solved by the direct methods via SHELXS-86.[29] Peak assignments were easily made in terms of both bond distances and peak heights. The serious absorption effects, from a linear absorption coefficient of 527.96 cm^{-1}, were corrected empirically according to, first, the average of the ψ-scan curves for three strong reflections at different θ values and, subsequently, by DIFABS (as recommended)[30] after the isotropic refinement converged (unnormalized transmission coefficient range = 0.60−1.30). Multiplicity refinements of Tl atoms with B's varying and the alkali-metal atom occupancies fixed indicated that the Tl sites are fully occupied with deviations from unity less than 3σ. The inverse procedure gave the same answer for alkali-metal atoms, and they were so fixed at unity thereafter. The refined secondary extinction coefficient was very small ($5(3) \times 10^{-10}$) and hence was not included in the final anisotropic refinement, which gave R, $R_w = 4.3$, 4.7% for 408 reflections $> 3\sigma_I$ and 30 variables. The highest residual peak in the final difference Fourier map was 2.50 e$^-$/Å^3, 1.58 Å from Tl2. All data reduction and structure refinements were performed using the TEXSAN package[31] on a VAX station.

Some data collection and refinement parameters are listed in Table 1, the atomic positional and isotropic equivalent thermal parameters are given in Table 2, and the important interatomic distances, in Table 3. More details as well as anisotropic displacement parameters are contained in the Supporting Information, and these as well as structure factor data are also available from J.D.C.

(25) Zintl, E. *Angew. Chem.* **1939**, *52*, 1. Klemm, W.; Busmann, E. *Z. Anorg. Allg. Chem.* **1963**, *319*, 297.
(26) Busmanov, V. D.; Yatsenko, S. P. *Russ. Metall.* **1981**, *5*, 157.
(27) Selwood, P. W. *Magnetochemistry*, 2nd ed.; Interscience Publishers: New York, 1956; p 70.
(28) Ashcroft, N. W.; Mermin, D. N. *Solid State Physics*; Holt, Rinehart, and Winston: Philadelphia, PA, 1976; p 649.
(29) Sheldrick, G. M. *SHELXS-86*; Universität Göttingen: Göttingen, Germany, 1986.
(30) Walker, N.; Stuart, D. *Acta Crystallogr.* **1986**, *A39*, 158.
(31) *TEXSAN*, Version 6.0 Package; Molecular Structure Corp.: The Woodlands, TX, 1990.

Table 3. Bond Distances in CsTl (<5.2 Å)

		Tl1	
Tl1−Tl1	3.434(3)	Tl1−Cs1	4.245(3)
Tl−Tl1	3.409(3)	Tl1−Cs2	4.064(4)
Tl1···Tl1[a]	4.836(3)	Tl1−Cs2	3.809(4)
Tl1−Tl2	3.026(3)	Tl1−Cs3	3.880(3)
Tl1−Tl2	3.089(3)	Tl1−Cs3	3.932(3)
Tl1−Cs1	4.075(4)		
		Tl2	
Tl2−Tl1	2 × 3.089(3)	Tl2−Cs2	2 × 4.181(3)
Tl2−Tl1	2 × 3.026(3)	Tl2−Cs3	3.747(4)
Tl2···Tl2[a]	3.741(5)	Tl2···Cs3[a]	2 × 4.6207(4)
Tl2−Cs1	2 × 4.412(3)		
		Cs1	
Cs1−Tl1	2 × 4.075(4)	Cs1−Cs2	2 × 4.818(2)
Cs1−Tl1	2 × 4.245(3)	Cs1−Cs2	2 × 4.6312(6)
Cs1−Tl2	2 × 4.412(3)	Cs1−Cs3	2 × 4.377(4)
Cs1−Cs1	2 × 4.702(3)	Cs1−Cs3	2 × 5.181(4)
		Cs2	
Cs2−Tl1	2 × 4.064(4)	Cs2−Cs1	2 × 4.818(2)
Cs2−Tl1	2 × 3.809(4)	Cs2−Cs2	2 × 4.953(4)
Cs2−Tl2	2 × 4.181(3)	Cs2−Cs3	2 × 4.145(3)
Cs2−Cs1	2 × 4.6312(6)		
		Cs3	
Cs3−Tl1	2 × 3.880(3)	Cs3−Cs1	2 × 4.377(4)
Cs3−Tl1	2 × 3.932(3)	Cs3−Cs1	2 × 5.181(4)
Cs3−Tl2	3.747(4)	Cs3−Cs2	2 × 4.145(3)
Cs3···Tl2[a]	2 × 4.6207(4)	Cs3−Cs3	3.902(8)

[a] Relatively long distances.

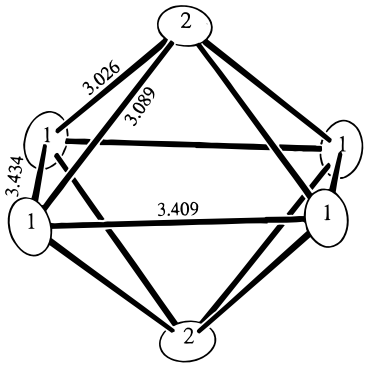

Figure 1. Isolated ~D_{4h} Tl_6^{6-} polyanion in CsTl. The actual symmetry is D_2 with 2-fold axes through apical Tl2 atoms and bisecting the *trans* edges of the Tl1 waist (50% probability thermal ellipsoids).

Results and Discussion

Cluster Skeleton. The main feature of the CsTl structure is the isolated compressed Tl_6^{6-} octahedral polyanion shown in Figure 1. The overall geometry is roughly similar to the squashed octahedron in KTl,[3] but the compression is more pronounced, and the waist of the octahedron is nearly square instead of the rectangular shape in KTl. The cluster has crystallographic D_2 symmetry (~D_{4h}) with the primary 2-fold axis through the apical Tl2 atoms, while the other two bisect trans edges in the Tl1 waist. The Tl−Tl separations around the octahedron range from 3.026(3) to 3.434(3) Å with an average of 3.179(3) Å, effectively the same as that in KTl (3.180(2) Å). The axial compression is illustrated by the relatively short *trans* Tl2−Tl2 distance, 3.741(5) Å versus 4.836(3) Å for the two Tl1−Tl1 diagonals. (The corresponding distances in KTl are 3.805(3) and 4.814(2) Å, respectively.) This accordingly divides the distances around the octahedron into two groups, the short 3.026(3) and 3.089(3) Å values for the eight Tl1−Tl2 edges and the long 3.409(3) and 3.434(3) Å within the expanded waist. The waist is essentially square (δ = 0.025(4) Å) in comparison with the more unequal Tl1−Tl1 bond lengths in KTl, 3.341(2) and 3.466(3)Å (δ = 0.125 Å). The absence of D_{4h} symmetry and the slight inequalities in the Tl1−Tl2 waist-to-apex distances originate from the nonplanarity of the waist Tl1 atoms, the *trans* pairs being separated from one another by ~0.10 Å. This is different from the situation in KTl where a 0.7° tilt of the Tl2−Tl2 axis from the normal to the waist rectangle further reduces the symmetry to C_{2h}. The cation environments appear to be largely responsible for these differences (below).

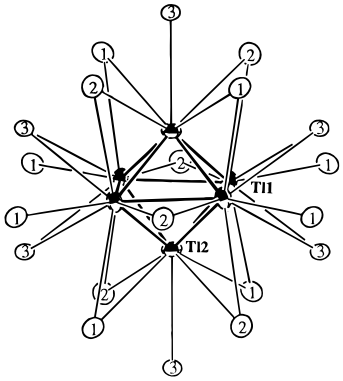

Figure 2. Distribution of cesium cations around Tl_6^{6-} with the same orientation as that in Figure 1. The dual bridging functions of Cs^+ ions are evident, and they are also coordinated to neighboring-like cluster units (50%).

Cation Distributions and Polyanion Packing. Analogous to KTl,[3] the isolated Tl_6^{6-} polyanions in CsTl are also sheathed by 20 alkali-metal cations to create the appropriate charge balance (Figure 2). Each octahedral edge is bridged by either a Cs1 or Cs2 atom except for the two longest Tl1−Tl1 edges, which are each μ_2-bridged by two Cs3 atoms (possibly the cause of the long edge). Each vertex also has an exo-cation, i.e., Cs1 to Tl1 and Cs3 to Tl2, respectively. Cs1 links four cluster units (exo-coordinated to two Tl1 and bridged to two Tl1−Tl2 edges), while Cs2 and Cs3 interconnect three clusters, with Cs2 bridged to one Tl1−Tl1 and two Tl1−Tl2 edges and Cs3 exo-bound to one Tl2 and bridged to two Tl1−Tl1 edges. Also noteworthy are the relatively short exo Cs3−Tl2 (3.747(4) Å) and Cs3−Cs3 (3.902(8) Å) distances. (As a comparison, the shortest Cs−Tl and Cs−Cs distances in Cs_8Tl_{11} are 3.816(2) and 4.286(3) Å, respectively.[5])

Figure 3 shows the space partitioning of polyanions and cations in the CsTl unit cell. Of particular interest is the different packing of anions (or polyanions) within the ATl (A = Na, K, Cs) series, which changes from a diamond-like face-centered-cubic pattern of thallium in NaTl (Figure 4) to an approximately face-centered arrangement of Tl_6^{6-} units in KTl[3] and then returns to an interpenetrating but only approximate face-centered array of Tl_6^{6-} units in CsTl. Note the resemblance of lattice constants between KTl (*Cmca*, a = 15.329(4) Å, b = 15.069(4) Å, and c = 8.137(2) Å) and CsTl (*Fddd*, a = 32.140(3) Å, b = 15.136(1) Å, and c = 9.2400(7) Å); a is approximately doubled in CsTl, while the other two remain roughly the same (scaled according to the larger size of Cs). The structure of KTl can be roughly viewed as the compressed version of CsTl after removal of every other Tl_6^{6-} layer along the a direction (or removal of one of the interpenetrating face-centered sublattices). This last feature of CsTl can be recognized better in the cell view in the synopsis (Table of Contents) which is drawn with an improper origin at ($^1/_8$, $^1/_8$, $^5/_8$).

Although there are some similarities between KTl and CsTl regarding both the cation distributions around Tl_6^{6-} clusters and local coordination environments around each individual atom, the packing of the Tl_6^{6-} polyanions is different, evidently

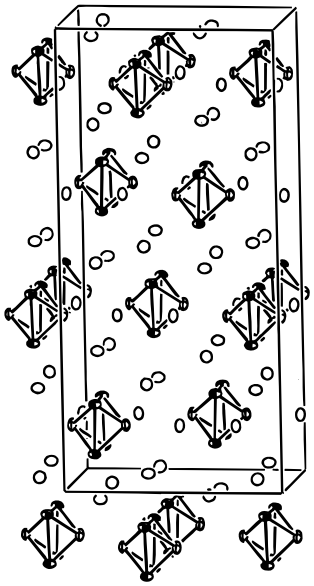

Figure 3. Approximate [001] view of the unit cell for CsTl showing isolated octahedral clusters in a diamond-like pseudo-*ccp* packing. The 50% probability ellipsoids are shaded for Tl1, crossed for Tl2, and open for Cs. The *b* axis and the compression axis of the cluster (through Tl2) lie horizontally.

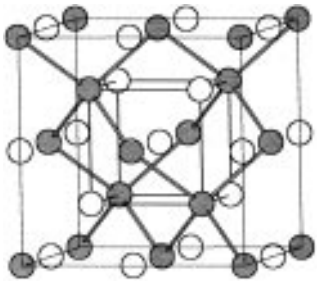

Figure 4. Unit cell view of NaTl showing the tetrahedrally coordinated diamond-like thallium network. Solid circles stand for Tl and open circles for Na. The alternate origin on Tl ($^1/_2$,0,0) is used for this representation.

because of different cation sizes. The principal differences lie in the environments around the Cs3 vs K3 atoms shown in Figure 5 and the unusual functionalities of A3 cations in connecting the adjacent Tl_6^{6-} units along the *bc* direction. The Cs3 pairs in CsTl and the K3 chain in KTl are the main distinction (although they are not really pairs or chains because there are also other alkali-metal neighbors around them). In CsTl, all of the cluster units have exactly the same orientation with the Tl2−Tl2 axes all along the *b* direction (Figure 3, top of Figure 5). The same 2-fold axis goes through both Tl2 and Cs3 atoms. A Tl2···Tl2 separation between two neighboring octahedra of 11.401(1) Å correlates with the two relatively short exo Cs3−Tl2 (3.75 Å) and Cs3−Cs3 (3.90 Å) distances. The shorter exo Cs3−Tl2 distances are consistent with the fewer Tl near neighbors around Cs3, 5 versus 6 for Cs1 and Cs2. The Tl2−Cs3 bonds are intrinsically shorter and stronger because of otherwise poorer packing about the compressed cluster; Tl2 is somewhat withdrawn from the best position for good cation solvation and shows a distinctly poorer Coulomb energy.

On the other hand, a mirror plane is shared by Tl2 and K3 atoms in KTl, so these atoms are allowed to twist with respect to each other to avoid too short distances (or to attain better cation solvation), resulting in two types of octahedron orientations with an ∼40.6° tilt from each other (bottom of Figure 5). Such deformation naturally creates anisotropic exo-bonding of K3 to Tl2 and thus leads to the 0.7° tilt of the Tl2−Tl2 axis

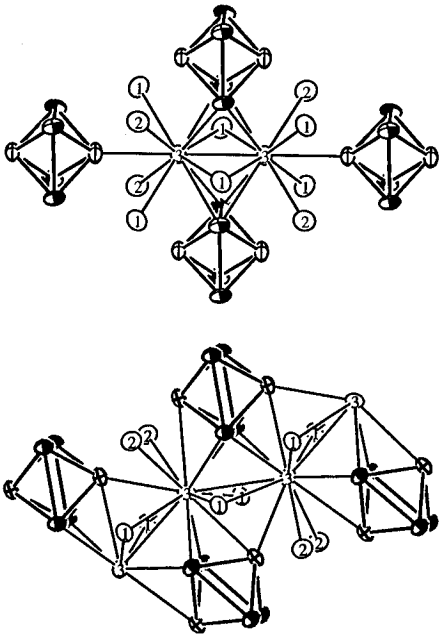

Figure 5. Comparison of the environments around A3 cations: (top) the Cs3 pair in CsTl; (bottom) the equally spaced zigzag K3 chain in KTl.

from the normal to the Tl1 rectangle. In CsTl, the larger size and lower field of Cs apparently afford a Tl_6^{6-} unit with a nearly square waist relative to the rectangular KTl. The ∼0.10−Å variation in the separation between the *trans*-pairs of Tl1 within the base of Tl_6^{6-} may be related to the asymmetric solvating character of Cs1 and Cs2, particularly on the Tl1−Tl2 waist-to-apex bonds (Figure 2). The two additional cation neighbors about Cs1 with respect to Cs2 (16 vs 14) together with its consistently longer distances to Tl neighbors (Table 3) probably leave it more positive, and this evidently leads to a shift of the waist Tl1 atoms toward the Cs1-bridging side. Since the size of Rb falls between those of K and Cs, the absence of a RbTl phase is peculiar. This might be related to either the inability to form an intermediate to a KTl- or CsTl-type structure without poor cation solvation and anion bonding or to an overwhelming stability of the high-melting Rb_8Tl_{11} phase.

Tl_6^{6-} Compression. The four other examples of main-group octahedral clusters are all *closo* deltrahedra and follow the Wade's ($n + 1$) orbital rule,[32] that is, with 14 electrons involved in skeletal (p orbital) bonding.[18−22] The hypoelectronic Tl_6^{6-} cluster has undergone a Jahn−Teller distortion with pronounced axial compression, one of the pathways which serve to reduce the cluster charge and stabilize the ion. This conclusion is supported by the results of extended Hückel calculations[33] on the isolated cluster shown in Figure 6. Transformation of the regular octahedral Tl_6 (d(Tl−Tl) = 3.28 Å, as observed in $Na_{14}K_6Tl_{18}Mg$[12]), to the tetragonally compressed model (D_{4h}) splits the high-lying t_{1u} skeletal orbital into e_u and a_{2u} and provides the major stabilization energy of distortion. The a_{2u} MO, which follows p_z and has dominant contribution from two apical Tl2 atoms, is σ bonding between the axial atoms and the square, but the compression leads to an increased π^* effect between the same atom pairs, a loss of π within the enlarging waist, and a strongly antibonding Tl2−Tl2 interaction along the compression axis. These effects drive a_{2u} higher in energy, actually to an antibonding state in accordance with its

(32) Wade, K. *Adv. Inorg. Chem. Radiochem.* **1976**, *18*, 1.
(33) Hoffmann, R. *J. Chem. Phys.* **1963**, *39*, 1397. The atomic parameters for Tl in the EHMO calculations were as follows: 6s $\zeta = 2.14$, $H_{ii} = -11.60$ eV; 6p, $\zeta = 2.04$, $H_{ii} = -5.80$ eV.[3]

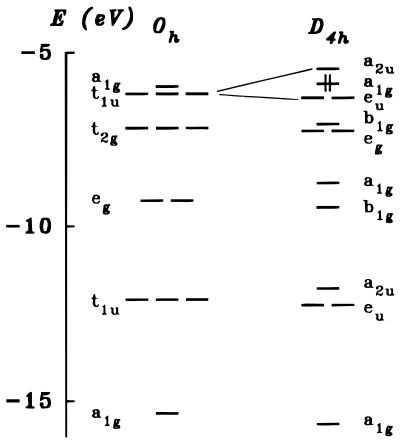

Figure 6. Extended Hückel results for the regular octahedral Tl_6^{8-} (O_h, d(Tl−Tl) = 3.28 Å) in $Na_{14}K_6Tl_{12}M$ (M = Mg, Zn)[12] and the tetragonally compressed Tl_6^{6-} (D_{4h}) in CsTl with suitable averages of the observed distances.

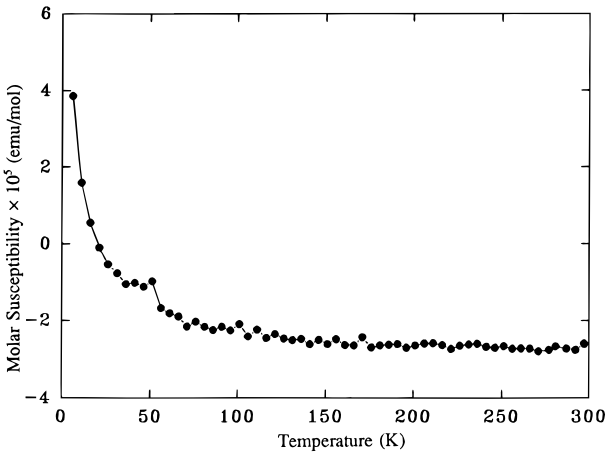

Figure 7. Temperature dependence of the molar susceptibility of CsTl over 6−300 K at 3 T. The tiny cusp around 50 K is probably related to traces of an external oxygen impurity. The noise originates largely because of the small signal observed.

negative overlap population. Evidently the $(e_u)^4(a_{1g})^2(a_{2u})^0$ configuration is energetically more favorable than the $(t_{1u})^6(a_{1g})^0$ alternative, which could otherwise result in a regular octahedron but with loss of bonding and without any orbital energy reduction. We presume the absence of the truly octahedral cluster in a Cs_4Tl_3 (Cs_8Tl_6) phase originates with an insufficiently stable packing of ions in these proportions. The MO diagram in Figure 6 is visually indistinguishable from that given earlier for the KTl analogue, even though the latter cluster is distorted appreciably toward D_{2h} and the calculation started with an idealized rather than observed octahedron. Inclusion of Tl 5d orbitals in the earlier calculations on KTl made no difference at all, presumably because these are both significantly contracted and more tightly bound. Although the levels in Figure 6 readily sort into six predominately p-based eigenstates above six that are largely s in character, as we have usually observed in other cases, appreciable s−p mixed is also present, as implied by the distribution of energies found.

The closed-shell electronic structure of the Tl_6^{6-} ion and the localized nature of the bonding in solid CsTl were confirmed, first, by the magnetic susceptibility measurement (Figure 7), which yielded a temperature-independent, weakly diamagnetic behavior, $\chi_M = -2.7(1) \times 10^{-5}$ emu/mol ($-0.48(2) \times 10^{-6}$ emu/cm^3) over 50−300 K after diamagnetic corrections for the atomic cores (-6.5×10^{-5} emu/mol)[25] and the cluster skeletal electrons (Langevin term, -1.4×10^{-5} emu/mol),[26] and, second, by the electrical measurements on several well-formed crystals with a two-probe dc technique, which gave a room temperature resistivities of $\sim 10^6$ $\mu\Omega$·cm, typical of a semiconductor (or a *very* poor metal). The dark grey color of the crystals is consistent with the semiconducting property because crystals are neither transparent (insulator) nor shiny (metal or small gap semiconductor).

Why Not NaTl-Type Structures? The stuffed diamond structure of NaTl is shown in Figure 4 as a superstructure of the *bcc* lattice.[24] It was for this compound that Zintl first explained the structure and bonding of polar intermetallic compounds in terms of simultaneous ionic and covalent pictures,[24,25] which was later called *the Zintl concept* by Laves.[34] Instead of applying Hume-Rothery's idea of a valence electron concentration,[35] Zintl proposed general electron transfer from the electropositive to the electronegative atoms (ionic part) and related several anionic substructures to known isoelectronic elemental structures (covalent part). In this case, Tl^- in NaTl is isoelectronic with carbon, which correlates with the diamond-like substructure. The covalent polyanionic framework is formed because the electrons from electropositive atoms are not sufficient to complete the octet of electronegative main-group elements. In order to reach a closed-shell configuration, the electronegative atoms instead have to share electrons with each other, forming homonuclear cluster or network structures.

While favorable bonding among anions is important in formation of a structure, cation solvation (A−Tl interactions) appears critical in determining which structures are formed. The stuffed diamond NaTl structure is favored (or allowed) because Na and Tl happen to have similar atomic sizes to satisfy both cation solvation and anion bonding requirements (the Na:Tl radius ratio is close to 1).[36] The 3.24 Å distance required for both Na−Tl and Tl−Tl contacts in NaTl falls in the range typically seen in the system, e.g., 3.13−3.62 Å (Na−Tl) and 3.18−3.30 Å (Tl−Tl) in Na_2Tl[2] as well as 3.13−3.25 Å (Na−Tl) and 3.21−3.42 Å (Tl−Tl) in $Na_4A_6Tl_{13}$ (A = K, Rb, Cs).[10] However, with a smaller Li or a larger K, Rb, or Cs, either cation solvation or anion bonding cannot be effectively fulfilled. Assuming that the overall structural pattern is governed by the conventional packing of the larger component, a hypothetical NaTl model for LiTl would result in inappropriately long Li−Tl distances (3.24 Å versus the range of 2.7−3.0 Å observed in binary Li−Tl phases[37]) or, more likely, a substantial rearrangement. In other words, the Tl:Li radius ratio is large and would require the Tl sublattice be significantly compressed in a well-bonded interpenetrating diamond-like structure.[36] The pressure-favored metallic CsCl-type structure emerges instead for LiTl with more Li−Tl (2.95 Å) and Tl−Tl (3.44 Å) interactions in a three dimensional framework.[23,38] Alternatively, in order to form a NaTl-type structure, the size of the anion would need to be reduced to match the size of the cation, which is exactly what happens for LiAl, LiGa, and LiIn.[39,40] Such observations have also been supported by high-level electronic structure calculations, which indicate that a NaTl-type structure is energetically preferred to a CsCl-type structure

(34) Laves, F. *Naturwissenschaften* **1941**, *29*, 244.
(35) Hume-Rothery, W. *Electrons, Atoms, Metals, and Alloys*, 3d ed.; Dover Publications: New York, 1963.
(36) Pearson, W. B. *The Crystal Chemistry and Physics of Metals and Alloys*; Wiley-Interscience Publishers: New York, 1972; pp 576−578.
(37) Li_2Tl: Stöhr, J.; Müller, W.; Schäfer, H. *Acta Crystallogr.* **1981**, *37A*, C-185. Li_3Tl and Li_5Tl_2: Stöhr, J.; Schäfer, H. *Z. Naturforsch.* **1979**, *34B*, 653.
(38) Christensen, N. E. *Phys. Rev.* **1985**, *B32*, 207.
(39) Kishio, K.; Brittain, J. O. *J. Phys. Chem. Solids* **1979**, *40*, 933.
(40) Zintl, E.; Woltersdorf, G. *Z. Elektrochem.* **1935**, *41*, 876.

when the sizes of the constituent atoms are nearly identical.[38,41] (These calculations also gave overlapping band structures at E_F, consistent with the metallic properties observed for all NaTl-type compounds.)

Similar considerations also apply to phases with larger cations, e.g., KTl and CsTl. A NaTl model for KTl or CsTl would result in Tl−Tl distances that are too long (>3.75 Å), tending toward the formation of unfavorably isolated Tl^- ions (isolated thallium atoms appear only as formal Tl^{5-} ions, as found in $Na_{23}K_9Tl_{15.33}$7 and $LiMg_2Tl$[42]). In other words, the K:Tl radius ratio is too large for suitable Tl−Tl contacts to be formed by compression of the K sublattice. Thus, the atoms must reposition themselves in space. A pattern with obviously effective cation solvation and good polyanion bonding is exemplified by orthorhombic *Cmca* for KTl and *Fddd* for CsTl, both with isolated, compressed octahedral Tl_6^{6-} polyanions, although we are naturally not able to exclude other structural possibilities *a priori*. Note that every Tl atom in KTl and CsTl is also 4-bonded (4b) to other Tl atoms ($\bar{d}$ = 3.18 Å), topologically equivalent to 4b−Tl^- in NaTl (3.24 Å), but not in the prototypical structure. Although the anion substructure is no longer related to those of an isoelectronic element, the spirit of the Zintl concept remains useful in guiding chemical synthesis and understanding structures in broader ranges of systems, especially after the concept is generalized (e.g., Zintl ions[43]) to include cluster structures with delocalized but closed-shell bonding.[25,44−46]

Three conclusions can be drawn from the above discussion. First, it is both the electronic factors (anionic bonding) and packing requirements (cation solvation) that determine the unique structures of the ATl (A = Li, Na, K, or Cs) phases. Second, the axial compression of the Tl_6^{6-} octahedron is solely driven by the limited number of valence electrons available for the octahedral cluster bonding in ATl compositions. And third, the differences in polyanion packing, axial compressions and waist distortions between KTl and CsTl are only related to the size factors of cations and their packing requirements. However, there are many other examples that would seem to follow size factors and electronic requirements but just do not work out. For instance, efforts made to tune the one-electron-deficient anions in $Na_4A_6Tl_{13}$ (A = K, Rb, Cs) to a closed-shell structure with M-centered icosahedral $Tl_{12}M^{10-}$ (M = Ge, Sn, or Pb) have so far all failed. This, together with the absence of a RbTl phase in the ATl system, show that satisfying electronic and packing requirements is not a sufficient condition for a phase to occur. The much more complex matter of phase stability ultimately plays the key role in determining the final products. And it is this unpredictable character that makes the synthesis of new materials fascinating and challenging.

Acknowledgment. We thank J. Ostenson for the measurements of magnetic susceptibility data.

Supporting Information Available: Tables of data collection and refinement details and of anisotropic displacement parameters for CsTl (2 pages). Ordering information is given on any current masthead page.

IC951265V

(41) Schmidt, P. C. *Phys. Rev.* **1985**, *B31*, 5015.
(42) Ramsey, W. J. *Acta Crystallogr.* **1965**, *18*, 817.
(43) Corbett, J. D. *Chem. Rev.* **1985**, *85*, 383.
(44) Schäfer, H. *Annu. Rev. Mater. Sci.* **1995**, *15*, 1.
(45) Nesper, R. *Prog. Solid State Chem.* **1990**, *20*, 1.
(46) Hughbanks, T. In *Inorganometallic Chemistry*; Fehlner, T., Ed.; Plenum Press: New York, 1992; p 291.